Journal of Food Engineering 147 (2015) 8–13

Contents lists available at ScienceDirect

Journal of Food Engineering

journal homepage: www.elsevier.com/locate/jfoodeng

Confocal imaging to reveal the microstructure of soybean processing materials

Katherine E. Preece [a,b,*], Ellen Drost [a], Nasim Hooshyar [a], Ardjan Krijgsman [a], Philip W. Cox [b], Nicolaas J. Zuidam [a]

[a] Unilever R&D Vlaardingen, Olivier van Noortlaan 120, 3133 AT Vlaardingen, The Netherlands
[b] School of Chemical Engineering, University of Birmingham, Edgbaston B15 2TT, United Kingdom

ARTICLE INFO

Article history:
Received 24 June 2014
Received in revised form 12 September 2014
Accepted 13 September 2014
Available online 22 September 2014

Keywords:
Aqueous extraction
Confocal laser scanning microscopy
Soy proteins
Sustainability

ABSTRACT

Sustainable production of food products for human consumption is required to reduce negative impacts on the environment and to consumer's health. Soybeans are an excellent source of nutritive plant proteins; aqueous extraction yields part of the available oil and protein from the legume. Many studies have been conducted which detail the various processing parameters and their effects on the extraction yields, yet there is little data on the localisation of nutritive components such as oil and protein in the fibrous unextracted by-product. Here we show a novel confocal laser scanning microscopy investigation of soybean processing materials and the physical effects of thermal treatment on the materials microstructure upon aqueous extraction. Various features, more specifically oil, protein (including protein aggregation) and cell wall structures, are visualised in the fibrous by-product, soy slurry and soy extract, with their presence both in the continuous phase and within intact cotyledon cells. Thermal treatment reduced the protein extraction yield; this is shown to be a result of aggregated protein bodies in the continuous phase and within intact cotyledons cells. Knowledge of the processing material microstructures can be applied to improve extraction yields and reduce waste production.

1. Introduction

In recent years, sustainable food supply has become a prevalent topic for consumers, industry and the scientific community (Adams and Demmig-Adams, 2013; Aiking, 2011; Cakmak, 2002; Leiserowitz et al., 2006; Pimentel and Pimentel, 2003). With the world population projected to increase by 2.3 billion inhabitants by 2050, the need to address uncertain food supplies is required at this moment to prevent malnutrition in coming years (Bruinsma, 2009). Adams and Demmig-Adams (2013) approach the topic by considering it not a question of plant- versus meat-based diets causing the most undesirable environmental and health issues, but more the methods chosen for animal rearing or crop production which makes a greater contribution to sustainability. However, no consideration is given for the post-processing during food manufacture. Processing of food sources requires examination to yield the most value from land available for agriculture, which will be limited by urbanisation and water required for their production in the near future. To maximise the availability of nourishment for human consumption, the extraction of health-promoting components also requires optimisation.

Used for a broad range of products, the soybean crop is versatile, and produces good quality protein for human consumption (Masuda and Goldsmith, 2009). Aqueous extraction of components from soybeans is currently undertaken for the production of some soy-based products, such as soymilk and tofu. The most frequent aqueous extraction protocol involves the grinding of dried soybeans with hot aqueous solution prior to the removal of insoluble fibrous material, termed okara (Giri and Mangaraj, 2012). The protein extraction yield of the described process is less than desirable, with a large fraction, typically 25–40% (dry basis) of soy proteins being separated into the fibrous by-product, okara (Campbell et al., 2011; Kasai and Ikehara, 2005; O'Toole, 1999; Rosenthal et al., 1998). Most commonly usage of the by-product is not widely employed for human consumption due to the uneconomical resale value of soy fibre products. More sustainable processing for food production could result in nutritious material being used for human sustenance (Jankowiak et al., 2014), rather than exiting the process within a waste stream, not limited just to soy milk and tofu preparation.

* Corresponding author at: Unilever R&D Vlaardingen, Olivier van Noortlaan 120, 3133 AT Vlaardingen, The Netherlands. Tel.: +31 (0)10 460 5290.
E-mail address: katherine.preece@unilever.com (K.E. Preece).

http://dx.doi.org/10.1016/j.jfoodeng.2014.09.022
0260-8774/

The microstructure of the starting material for extraction, the soybean, has been well studied (Bair and Snyder, 1980; Horisberger et al., 1986; Lili et al., 2013; Rosenthal et al., 1998; Tombs, 1967). The soybean is mainly comprised of cotyledon cells; oval in shape, 15–20 μm in diameter and 70–80 μm long, and consisting of lipid and protein bodies, in the size ranges of 0.2–0.5 μm and 8–20 μm respectively (Rosenthal et al., 1998). The protein bodies account for 60–70% of the total soybean protein content, consisting of storage proteins glycinin and β-conglycinin, confirmed using an immunogold method (Horisberger et al., 1986). Techniques used to deduce the microstructure of soybeans, including electron microscopy and fluorescence microscopy, possess limiting factors, ranging from laborious sample preparation prior to visualisation and/or poor resolution, which prevent their routine use.

Previously studies to investigate ways to increase the extraction yields of health-promoting components from soybeans have been conducted (Giri and Mangaraj, 2012; Rosenthal et al., 1998; Vishwanathan et al., 2011). Yet there is a lack of understanding of the microstructure of processing materials which is crucial for achieving greater extraction yields. With this information, processing which targets the exposed restraints can be employed to improve their extraction yields. In this paper we show the location of oil and protein in soy extract, soy slurry and okara, alongside the effects of heat treatment using confocal laser scanning microscopy (CLSM).

2. Materials and methods

2.1. Materials

All extractions and microstructural investigations were carried out using commercially available soybeans from the same batch. Soybeans were stored in an airtight container prior to processing. All extractions were carried out using demineralised water, and resulting samples were stored at 4 °C before analysis. Fluorescent dyes for CLSM were purchased from various suppliers; acridine orange (Polysciences Inc., Warrington, PA), nile blue A (Janssen Chimica, Belgium) and rhodamine B (Merck, Germany) were investigated.

2.2. Sample preparation

To prepare soy processing materials, dried soybeans were coarsely ground in demineralised water at a soybean:water ratio of 1:6 (w/w) with a commercial blender (Varoma Thermomix, Vorwerk, Germany) (10 min, 80 °C (final temperature approximately 85 °C), levels 2–8 stepwise) and ground finely using a high shear mixer (Silverson L4RT, Silverson Machines International, UK) (20 min, 3000–6500 rpm stepwise (final temperature approximately 70 °C)) to produce a soy slurry. The resultant soy slurry (pH 6.5) was immediately centrifuged at 4249 × *g* for 10 min to separate the soy extract (pH 6.4) from the fibrous insoluble okara. To prepare soy milk soybeans are commonly extracted at temperatures between 80 and 100 °C to minimise lipid oxidation by enzymes and denature trypsin inhibitors (Giri and Mangaraj, 2012). Non-heat treated protein extraction was also carried out at ambient temperature as a control. After a total of 30 min grinding, the soy slurry increased to 41.4 °C as no temperature control was performed, which is well below the denaturation temperatures for the main storage proteins, β-conglycinin and glycinin (74–77 °C and 92–93.7 °C, respectively; Kinsella, 1979; Wang et al., 2014).

2.3. Determination of protein & moisture contents

Okara, soy extracts and soy slurry samples were analysed for protein concentration using the Dumas method (Vario MAX CNS, Elementar Analysensysteme GmbH, Germany) and L(+)-glutamic acid (VWR International BVBA, Belgium) as a standard (Jung et al., 2003). From the nitrogen content the protein concentration was calculated with a protein conversion factor of 6.25 × N. The extraction yields were determined using Eq. (1.1), where $mass_{p,se}$ is the mass of protein in the soy extract and $mass_{p,o}$ is the mass of protein found in okara.

$$\text{Protein extraction yield}(\%) = \frac{mass_{p,se}}{(mass_{p,se} + mass_{p,o})} \times 100 \qquad (1.1)$$

Protein concentrations are determined on a wet basis (w.b.). Moisture content was also determined for all samples using a microwave moisture analysis system (SMART System5, CEM GmbH, Germany).

All of the analytical measurements were carried out in triplicate for each sample, and reported as the mean ± standard deviation.

Table 1
Excitation & emission settings for dye stock solutions used for confocal laser scanning microscopy.

Dye	Excitation wavelength (nm)	Emission wavelengths (nm)	Corresponding colour in micrographs
1% w/v Acridine orange	488	497–556	Green
	561	569–646	Red
		655–724	Blue
1% w/v Nile blue	488	520–626	Green
	633	662–749	Red
0.5% w/v Rhodamine B	488	492–555	Green
		566–631	Red
		645–751	Blue

2.4. Particle size analysis

Particle sizes of samples were measured using laser diffraction techniques, using Mastersizer 2000 Hydro S (Malvern Instruments Ltd, UK). Refractive indices of 1.33 and 1.45 were used for the dispersant and particles respectively.

2.5. Confocal laser scanning microscopy (CLSM)

Soy microstructures were visualised by confocal microscopy using Leica TCS-SP5 coupled with DMI6000 inverted optical microscope (Leica Microsystems Inc., Germany). Fluorochromes were selected based on their affinity to associate with various components within the samples; acridine orange, nile blue and rhodamine B were shortlisted. The dyes concentrations in the stock solution, excitation and emission wavelengths, including the user set colours for emitted light, are shown in Table 1. For all samples, one drop of dye stock solution was added to 1–1.5 mL of sample and mixed well before slide preparation, which is less tedious and time consuming than previously reported techniques. The microscope is equipped with three lasers for excitation: an Argon laser ($\lambda_{excitation}$ 488 nm), a Diode-Pumped-Solid-State laser ($\lambda_{excitation}$ 561 nm) and a Helium-Neon laser ($\lambda_{excitation}$ 633 nm). For the visualisation of samples using nile blue, emission caused by the excitation laser is avoided by using sequential scanning. A 40 × oil immersion objective (1.25 NA) was utilised for visualisation of all materials.

3. Results and discussion

Acridine orange was used to visualise a soy slurry sample using confocal microscopy; Fig. 1 shows a representative micrograph. Intact cotyledon cells are present within soy slurry containing intact intracellular material: areas emitting purple in colour, a

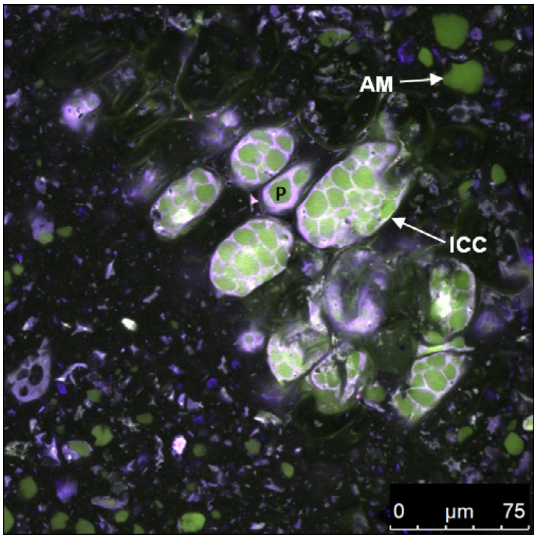

Fig. 1. Representative confocal laser scanning micrograph of soy slurry sample obtained after grinding at 80 °C with acridine orange. Examples of intact cotyledon cells (ICC), protein bodies within cotyledon cells (P, green) and agglomerated material (AM, green) are annotated on the image. Fibrous material appears as a combination of blue and red emission, i.e. purple. (For interpretation of the references to colour in this figure legend, the reader is referred to the web version of this article.)

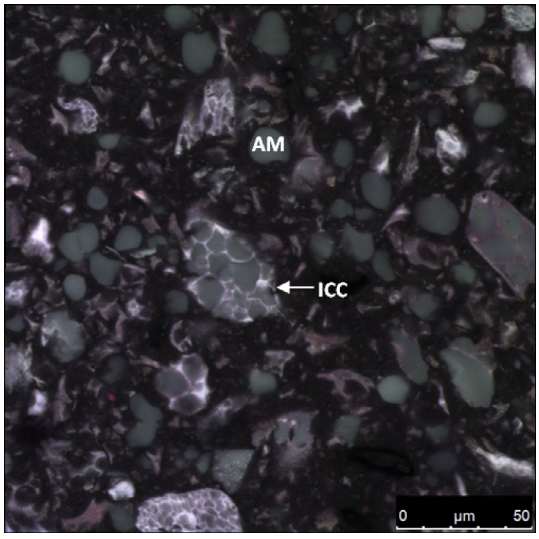

Fig. 2. Confocal micrograph of soy slurry with preparation including thermal treatment (80 °C), stained using rhodamine B. Examples of agglomerated material (AM) and intact cotyledon cells (ICC) are labelled in the figure. Proteinaceous material is highlighted using this fluorochrome.

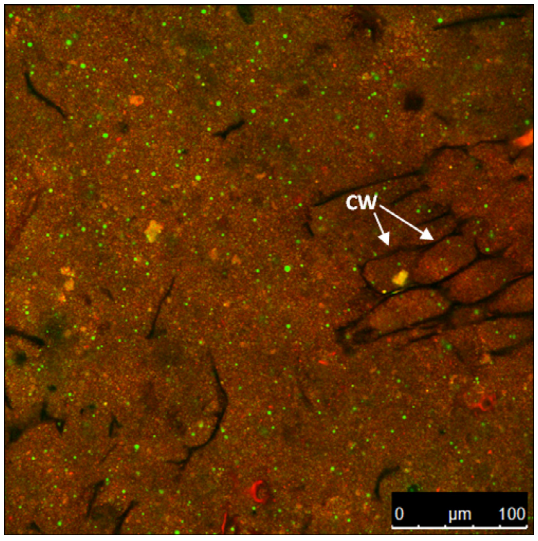

Fig. 3. Confocal micrograph of soy slurry prepared at ambient temperature, stained with fluorochrome nile blue. Oil is represented in the colour green and other apolar material, including protein, in red or orange (a combination of red and green). Examples of cotyledon cell wall material (CW, black lines) are annotated on the image. (For interpretation of the references to colour in this figure legend, the reader is referred to the web version of this article.)

combination of blue and red, are the oleosins around oil bodies and areas emitting green are protein bodies. Similar structures found within soybean flour were observed by transmission electron microscopy (TEM) (Campbell and Glatz, 2009). In the extraction medium (outside the intact cells), agglomerated material depicted in green was observed within the size range approximately 5–20 µm. The wavelength at which the material in the aqueous medium emits fluorescence (497–556 nm, green), and also their size both suggest that the material consist of aggregated protein bodies. To confirm that the agglomerated material in the continuous phase were not starch granules; iodine solution was used in conjunction with light microscopy. No significant purple-black staining of the observed extracellular features occurred when examined using light microscopy, confirming the material was not starch (data not shown). However, it is important not to neglect that starch grains are present within the soybean (He et al., 2007), and subsequently starch should be present in the soy slurry. A number of extracellular materials can be visualised in the aqueous medium and within intact cotyledon cells using acridine orange.

To verify the composition of agglomerated material observed in the soy slurry using acridine orange (Fig. 1), a dye specifically used to label proteins was explored; rhodamine B. Agglomerated material was visualised in soy slurry when rhodamine B was employed for protein localisation, shown in Fig. 2. Protein within intact cotyledon cells was also revealed using rhodamine B; rhodamine B associated with aggregated material in the aqueous medium was shown to emit fluorescence at the same wavelength as dye associated with protein bodies located within the cells. The use of rhodamine B further confirms the agglomeration of protein in- and outside the cotyledon cells when the soy slurry was thermally processed.

Nile blue is primarily used as a lipid stain; lipids are also considered an important substituent of soybeans when performing an extraction (Rosenthal et al., 1998), which are not visualised using acridine orange or rhodamine B due to their poor solubility in oil. In Fig. 3, lipids are depicted green and other apolar material red or orange in the soy slurry prepared at room temperature. Clusters of cell wall material were present in the soy slurry which appears to contain only aqueous media; protein and oil were extracted. During grinding of the soybeans, the cell wall is disrupted which exposes the intracellular components from within the cell to the aqueous medium for diffusion of the internal components into the extraction medium (Campbell and Glatz, 2009). The agglomerated material in the size range 5–20 µm presented in Figs. 1 and 2 are absent using nile blue in the soy slurry when extraction was performed at ambient temperature (Fig. 3).

Agglomerated material (most likely protein bodies) as shown in Figs. 1 and 2 are also visible in Fig. 4 (depicted in red), which is obtained by CLSM of a soy slurry prepared at 80 °C and visualised with nile blue. The agglomerated material is surrounded by green dots which are most likely liberated oil bodies. It has been suggested before that heating whilst grinding aqueous soy slurry

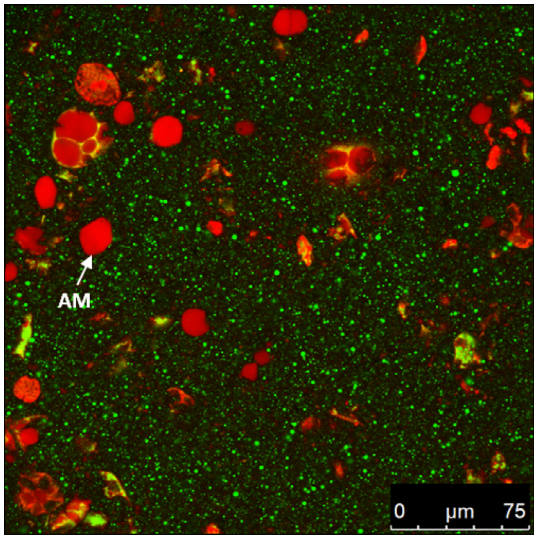

Fig. 4. A representative confocal micrograph of soy slurry with preparation including thermal treatment (80 °C) visualised with nile blue. Oil is presented in green and agglomerated material within the heat treated sample (also labelled AM), is depicted in red. (For interpretation of the references to colour in this figure legend, the reader is referred to the web version of this article.)

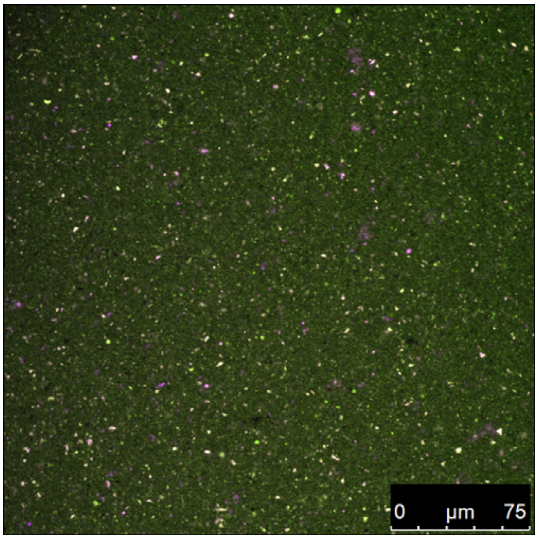

Fig. 5. Representative confocal micrograph of soy extract obtained at 80 °C visualised using fluorochrome acridine orange. (For interpretation of the references to colour in this figure legend, the reader is referred to the web version of this article.)

causes proteinaceous material to aggregate due to denaturation (Nishinari et al., 2014). Thermal denaturation of the main storage proteins β-conglycinin and glycinin occurs in the ranges 74–77 °C and 92–93.7 °C respectively, which accounts for aggregation when soybeans were ground at 80 °C (Kinsella, 1979; Wang et al., 2014). Aggregation of supernatant protein of a size less than 40 nm occurs upon heating of soymilk to increase the concentration of protein particles in the size range 40–110 nm (Ono et al., 1991). The present study suggests that the protein bodies already aggregate prior to protein solubilisation in the aqueous phase at 80 °C, as their size did not change.

Approximately 26% more protein is extracted into the soy extract when no thermal treatment is applied compared to extraction at 80 °C in this present study (Table 2), which has also been observed in the literature (Campbell et al., 2011; Johnson and Synder, 2014; Rosenthal et al., 1998). The difference in protein extraction yields is not due to differences in particle sizes ($D_{4,3}$ and $D_{3,2}$) as the efficiency of grinding is not extensively affected by thermal treatment (Table 3). One may assume that only cells which are broken release their (protein) content. Campbell et al. (2011) suggested that for complete extraction to occur, the particle size needs to be in the size range of individual cotyledon cells, which assumes all cells are broken. It was assumed that only soybean cells on the outside of milled flour are disrupted resulting in a lower extraction yield with larger particle sizes of the milled flour. This was not the case when observing soy slurry in the present study; intact cotyledon cells were normally found singularly (see Figs. 1–4 and 6). With combined flaking and pin milling of soybeans approximately 95% of cotyledon cells were disrupted when 57% of the total flour volume was made up of particles smaller than 55 µm, as confirmed using microscopy (Campbell and Glatz, 2009).

The soy extract obtained after the removal of okara did not contain the aggregated protein bodies. Fig. 5 shows the presence of only small (<5 µm) colloidal material homogenously dispersed throughout the aqueous environment, with fragmented fibrous material also visible. The absence of the agglomerated material in the soy extract after separation of insoluble material could be used to explain the reduced protein extraction upon thermal treatment (Table 2). However, aqueous extraction from soybeans at an elevated temperature is essential for the production of a

Table 2
Summary of protein extraction yield, protein solubility and predicted yields by [b]Campbell and Glatz (2009) and [c]Rosenthal et al. (1998).

Processing conditions	Protein extraction yield (%)	Total protein solubilised (%)[a]	Predicted protein extraction yield[b] (%)	Predicted protein extraction yield[c] (%)
Ambient temperature grinding	67.3 ± 1.9	89.7 ± 1.9	70.3 ± 2.2	74.3 ± 0.1
80 °C grinding	41.5 ± 0.2	64.9 ± 0.2	70.9 ± 2.2	63.8 ± 0.6

[a] The total protein solubilised was calculated assuming all moisture within okara has the same protein content as soy extract.
[b] Volume-weighted mean diameter ($D_{4,3}$) from Table 3 was used for calculations.

Table 3
Soy slurry processing conditions and resulting extraction yield and concentration of protein within the by-product, okara.

Processing conditions	Particle size		Soy extract		Okara	
	$D_{4,3}$ (µm)	$D_{3,2}$ (µm)	Protein content (w.b.) (%)	Water content (%)	Protein content (w.b.) (%)	Water content (%)
Ambient temperature grinding	330.8 ± 16.6	17.5 ± 1.0	3.6 ± 0.3	90.0 ± 0.1	4.7 ± 0.04	81.2 ± 0.1
80 °C grinding	267.8 ± 24.3	20.9 ± 1.9	3.4 ± 0.02	91.7 ± 0.6	7.3 ± 0.3	79.7 ± 0.6

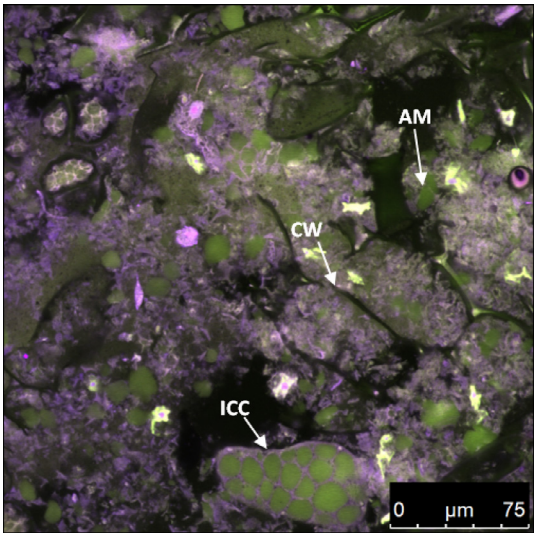

Fig. 6. CLSM micrograph of fibrous by-product of soy extract production at 80 °C, okara, visualised using acridine orange. Intact cotyledon cells (ICC), cell walls of disrupted cells (CW) and agglomerated material (AM in green, most likely protein bodies) are annotated on the image. Fibrous material appears as a combination of blue and red emission, i.e. purple. (For interpretation of the references to colour in this figure legend, the reader is referred to the web version of this article.)

flavoursome and safe final product due to the prevention of the enzyme lipoxygenase and trypsin inhibitors actions (Nik et al., 2009).

Fig. 6 depicts the microstructure of okara produced using thermal processing and stained with the fluorochrome acridine orange. Cell wall material and intact cells are observed that were present in the soy slurry prior to separation. Agglomerated material can be observed in the micrograph which have the same size and colour as seen in Fig. 1 in the continuous phase. Next to the removal of the protein aggregates during separation of the fibrous by-product okara, the loss in protein extraction yield can also be caused by the high moisture content of okara, approximately 80%; the cell walls of disrupted cells possess a robust difficult to compress network (see Table 3).

Campbell and Glatz (2009) proposed a model based on particle size and assuming that only soybean cotyledon cells on the outside are disrupted (discussed above). Another model by Rosenthal et al. (1998) was built up from the mass balance, where it was assumed that the protein concentration at equilibrium can be related to the one in the 'solid' phase by a partition coefficient. Despite the differences in models and our finding that we could not confirm the assumption of Campbell and Glatz (2009) that only the outside of soybeans cells are disrupted (see above), the calculated yields of the proteins using these two models and our values were similar to these found experimentally at ambient temperature (see Table 2). When examining the predicted yields for processing at 80 °C (between the denaturation temperatures of the main storage proteins), the calculated yields were much larger than actually found, as insolubility due to protein aggregation was not considered within either model. Table 2 shows indeed that the solubilities of 90% versus 65% for ambient and 80 °C processing respectively, is mainly responsible for the differences in extraction yield.

Okara produced using thermal treatment contains 2.6% more protein than when no thermal treatment was employed. The proteins located within okara after thermal treatment are found to possess good nutritive value, therefore could be extracted for human consumption (Stanojevic et al., 2012). The aqueous phase within the okara may have the same composition as the soy extract; if more of it is removed from okara, the protein extraction yield will be increased.

SEM was a technique investigated for this study as well; yet limited information was obtained from it. Similar SEM images as already published of frozen soybeans (Bair and Snyder, 1980) were obtained (data not shown). Intact protein bodies were observed which coincides with findings from CLSM. SEM with energy dispersive spectroscopy (EDS) was also used to confirm the composition of aggregated material found in the continuous phase. Nitrogen was difficult to detect using this technique due to its low atomic number, especially with the concentrations found within the soy slurry; however it was detectable for some images of okara (data not shown). Although our SEM images in combination with EDS confirmed the composition of the aggregated material, it provided less informative insights and overall view relevant for the extraction process than CLSM. Moreover, SEM is a more tedious and time consuming technique than CLSM and the structures might also be affected by the freezing prior to SEM analysis.

Localisation of protein within the by-product is important for looking at methods for protein recovery; the avoidance of protein insolubility is one method to target increased protein extraction. Enzymatic treatment to reduce rigidity of the disrupted cell wall matrix has shown promising results for improved oil and protein extraction yields, and could be one approach to target extraction from the by-product okara (Kasai et al., 2004; Rosenthal et al., 2001).

4. Conclusions

In this novel study we have shown the microstructures of soy slurry, soy extract and the fibrous waste material okara, including localisation of oil and protein using CLSM in combination with carefully selected fluorochromes. Agglomerated protein bodies caused by thermal treatment were found in- and outside intact cotyledon cells in the soy slurry, and after separation in the okara only. Protein aggregation can be used to explain why a higher protein extraction yield was obtained upon processing at ambient temperature than after processing at 80 °C (67% versus 42% respectively). Treatments to disrupt the complex okara microstructure and/or achieve lower water content will be investigated in further studies with the aim of increasing the protein extraction yield.

Acknowledgements

The authors would like to thank Clive Marshman and Richard Greenwood for their contributions to the project. The authors would like to acknowledge the Engineering & Physical Science Research Council (EPSRC) for partially funding this project.

References

Adams, R.B., Demmig-Adams, B., 2013. Impact of contrasting food sources on health versus environment. Nutr. Food Sci. 43, 228–235.
Aiking, H., 2011. Future protein supply. Trends Food Sci. Technol. 22, 112–120.
Bair, C.W., Snyder, H.E., 1980. Electron microscopy of soybean lipid bodies. J. Am. Oil Chemists' Soc. 57, 279–282.
Bruinsma, J., 2009. The resource outlook to 2050: by how much do land, water and crop yields need to increase by 2050? In: FAO Expert Meeting on How to Feed the World in 2050, Rome, Italy.
Cakmak, I., 2002. Plant nutrition research: priorities to meet human needs for food in sustainable ways. Plant Soil 247, 3–24.
Campbell, K.A., Glatz, C.E., 2009. Mechanisms of aqueous extraction of soybean oil. J. Agri. Food Chem. 57, 10904–10912.
Campbell, K.A., Glatz, C.E., Johnson, L.A., Jung, S., De Moura, J.M.N., Kapchie, V., Murphy, P., 2011. Advances in aqueous extraction processing of soybeans. J. Am. Oil Chemists' Soc. 88, 449–465.
Giri, S.K., Mangaraj, S., 2012. Processing influences on composition and quality attributes of soymilk and its powder. Food Eng. Rev. 4, 149–164.
He, F., Huang, F., Wilson, K.A., Tan-Wilson, A., 2007. Protein storage vacuole acidification as a control of storage protein mobilization in soybeans. J. Exp. Botany 58, 1059–1070.
Horisberger, M., Clerc, M.F., Pahud, J.J., 1986. Ultrastructural localization of glycinin and +|-conglycinin in glycine max (soybean) cv. Maple arrow by the immunogold method. Histochemistry 85, 291–294.

Jankowiak, L., Trifunovic, O., Boom, R.M., Van Der Groot, A.J., 2014. The potential of crude okara for isoflavone production. J. Food Eng. 124, 166–172.
Johnson, K.W., Synder, H.E., 2014. Soymilk: a comparison of processing methods on yields and composition. J. Food Sci. 43, 349–353.
Jung, S., Rickert, D.A., Deak, N.A., Aldin, E.D., Recknor, J., Johnson, L.A., Murphy, P.A., 2003. Comparison of Kjeldahl and Dumas methods for determining protein contents of soybean products. J. Am. Oil Chemists' Soc. 80, 1169–1173.
Kasai, N., Ikehara, H., 2005. Stepwise extraction of proteins and carbohydrates from soybean seed. J. Agri. Food Chem. 53, 4245–4252.
Kasai, N., Murata, A., Inui, H., Sakamoto, T., Kahn, R.I., 2004. Enzymatic high digestion of soybean milk residue (okara). J. Agri. Food Chem. 52, 5709–5716.
Kinsella, J.E., 1979. Functional properties of soy proteins. J. Am. Oil Chemists' Soc. 56, 242–258.
Leiserowitz, A.A., Kates, R.W., Parris, T.M., 2006. Sustainability values, attitudes, and behaviors: a review of multinational and global trends. Ann. Rev. Environ. Res. 31, 413–444.
Lili, W., Yeming, C., Zaigui, L., 2013. The effects of freezing on soybean microstructure and qualities of soymilk. J. Food Eng. 116, 1–6.
Masuda, T., Goldsmith, P.D., 2009. World soybean production: area harvested, yield, and long-term projections. Int. Food Agribusiness Manage. Rev. 12, 143–162.
Nik, A.M., Tosh, S.M., Woodrow, L., Poysa, V., Corredig, M., 2009. Effect of soy protein subunit composition and processing conditions on stability and particle size distribution of soymilk. LWT-Food Sci. Technol. 42, 1245–1252.
Nishinari, K., Fang, Y., Guo, S., Phillips, G.O., 2014. Soy proteins: a review on composition, aggregation and emulsification. Food Hydrocol. 39, 301–318.
Ono, T., Choi, M.R., Ikeda, A., Odagiri, S., 1991. Changes in the composition and size distribution of soymilk protein particles by heating (food & nutrition). Agri. Biol. Chem. 55, 2291–2297.
O'Toole, D.K., 1999. Characteristics and use of okara, the soybean residue from soy milk production a review. J. Agri. Food Chem. 47, 363–371.
Pimentel, D., Pimentel, M., 2003. Sustainability of meat-based and plant-based diets and the environment. Am. J. Clin. Nutr. 78, 660S–663S.
Rosenthal, A., Pyle, D.L., Niranjan, K., 1998. Simultaneous aqueous extraction of oil and protein from soybean: mechanisms for process design. Food Bioprod. Process. 76, 224–230.
Rosenthal, A., Pyle, D.L., Niranjan, K., Gilmour, S., Trinca, L., 2001. Combined effect of operational variables and enzyme activity on aqueous enzymatic extraction of oil and protein from soybean. Enzyme Microbial. Technol. 28, 499–509.
Stanojevic, S.P., Barac, M.B., Pesic, M.B., Vucelic-Radovic, B.V., 2012. Composition of proteins in okara as a byproduct in hydrothermal processing of soy milk. J. Agri. Food Chem. 60, 9221–9228.
Tombs, M.P., 1967. Protein bodies of the soybean. Plant physiol. 42, 797–813.
Vishwanathan, K.H., Singh, V., Subramanian, R., 2011. Influence of particle size on protein extractability from soybean and okara. J. Food Eng. 102, 240–246.
Wang, Z., Li, Y., Jiang, L., Qi, B., Zhou, L., 2014. Relationship between secondary structure and surface hydrophobicity of soybean protein isolate subjected to heat treatment. J. Chem. 2014, 1–9.